Characteristics of selective oxidation during the fabrication of vertical cavity surface emitting laser

2006 Chinese Phys. 15 1806

(http://iopscience.iop.org/1009-1963/15/8/029)

Vol 15 No 8, August 2006
1009-1963/2006/15(08)/1806-04

Chinese Physics

Characteristics of selective oxidation during the fabrication of vertical cavity surface emitting laser

Hao Yong-Qin(郝永芹)[a], Zhong Jing-Chang(钟景昌)[a], Ma Jian-Li(马建立)[a], Zhang Yong-Ming(张永明)[b], and Wang Li-Jun(王立军)[c]

[a] *National Key Lab of High-Power Semiconductor Lasers, Changchun University of Science and Technology, Changchun* 130022, *China*

[b] *Material & Engineering College, Shenyang Institute of Chemical Technology, Shenyang* 110142, *China*

[c] *Changchun Institute of Optics, Fine Mechanics and Physics, Changchun* 130033, *China*

(Received 17 December 2005; revised manuscript received 2 February 2006)

Taking into account oxidation temperature, N_2 carrier gas flow, and the geometry of the mesa structures this paper investigates the characteristics of selective oxidation during the fabrication of the vertical cavity surface emitting laser (VCSEL) in detail. Results show that the selective oxidation follows a law which differs from any reported in the literature. Below 435°C selective oxidation of $Al_{0.98}Ga_{0.02}As$ follows a linear growth law for the two mesa structures employed in VCSEL. Above 435°C approximately increasing parabolic growth is found, which is influenced by the geometry of the mesa structures. Theoretical analysis on the difference between the two structures for the initial oxidation has been performed, which demonstrates that the geometry of the mesa structures does influence on the growth rate of oxide at higher temperatures.

Keywords: laser technique, selective oxidation, vertical-cavity surface-emitting laser, quantum-well, semiconductor laser

PACC: 4255P, 4265, 8160C

1. Introduction

Vertical cavity surface emitting lasers (VCSELs) have emerged as attractive light sources for various applications in optical communication, optical interconnects,[1] laser printing, and optical storage due to their low-cost fabrication and packaging, low drive currents, low divergence circular beams, and the possibility of integrating VCSELs in 1- and 2-D arrays for parallel links. Oxidation of the AlAs (or AlGaAs with high Al content) layer has evolved into a key technology in fabrication of high-performance VCSELs.[2−4] The oxide provides both current confinement and index guiding, and produces the lowest threshold[3] and highest efficiency[5,6] VCSELs ever reported.

There exists considerable controversy as to whether or not oxidation follows a linear or parabolic growth rate.[7−9] Linear growth rates were reported for selective oxidation of $Al_{0.98}Ga_{0.02}As$.[8] Meanwhile, it has been reported for selective oxidation of AlAs that the initial oxide growth is linear with time and converts to parabolic growth with increasing oxide thickness.[9] Alonzo *et al* reported the effect of cylindrical geometry on the wet thermal oxidation of AlAs, but they did not take into account temperatures. We have fabricated GaAs–AlGaAs VCSELs and characterized their static properties by using a perforated ring (PR) instead of a ring trench (RT) as the lateral oxidation window.[10] In this paper we employed partial oxidation of the $Al_{0.98}Ga_{0.02}As$ layer in the distributed Bragg reflector (DBR) mirror stack to form the current aperture. Characteristics of the selective oxidation are discussed in detail by taking into account oxidation temperature, N_2 carrier gas flow, and the geometry of the mesa structures, and our own results have been obtained.

2. Experiment

The VCSEL wafers used in this study were grown by molecular beam epitaxy (MBE) technique on n^+

GaAs substrates. The bottom Bragg reflector consisted of 34 n-type Si-doped $Al_{0.9}Ga_{0.1}As$/GaAs pairs with quarter-wavelength-thick layers. The active region contained a GaAs–AlGaAs based three-quantum-well in a one-wavelength cavity for 850nm emission. The top Bragg reflector consists of 24 p-type C-doped $Al_{0.9}Ga_{0.1}As$/GaAs pairs. A $Al_{0.98}Ga_{0.02}As$ layer used for the subsequent selective oxidation was placed in the fourth quarter-wavelength layers above the active region. Test wafers with similar structure were repeatedly grown and characterized by photoreflectance and photoluminescence spectroscopy until the precise growth conditions and epitaxial structure are achieved.

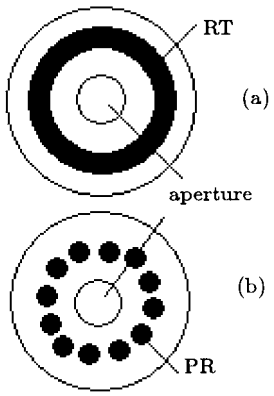

Fig.1. Sketches of mesas with RT and PR.

During fabrication of VCSELs, mesas with different geometry (RT and PR, shown in Fig.1) were defined by photoresist and etched by chemically assisted reactive ion beam etching (using Cl_2 /BCl_3) down to the active layer. The exposed $Al_{0.98}Ga_{0.02}As$ layer was oxidized at temperatures ranging from 350 to 458°C in the N_2/H_2O atmosphere. Dry N_2 with a constant flow of 1.4 liter per minute was used as carrier gas for H_2O vapour. The saturated N_2+H_2O gas was preheated in a capillary at the bottom of the quartz tube to ensure thorough adaptation to the applied oxidation temperature at the sample. In-situ thermal annealing was done in nitrogen environment for 50 min to reduce the dislocation and defects, also in favour of the removal of the volatile productions such as As and As_2O_3. A cross-section scanning electron micrograph of a selectively oxidized wafer is shown in Fig.2. No dislocation or other crystalline defects are apparent along the oxide–semiconductor interface or near the oxidation terminal.

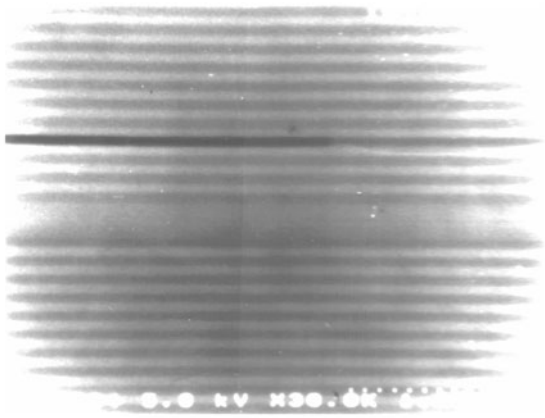

Fig.2. Cross-section scanning electron micrograph of a oxidized wafer.

3. Results and discussion

3.1. Growth dependence on time and temperature

The extent of the selective oxidation of a buried $Al_{0.98}Ga_{0.02}As$ layer within a DBR mirror is plotted in Fig.3 and Fig.4. They show the lateral oxidation depth w versus oxidation time t at temperatures ranging from 350 to 458°C. An approximately linear behaviour of the oxidation depth dependence of time is observed for lower temperatures (below 435°C), which is in agreement with Ref.[8]. The oxidation rate of mesas with RT is about 1.5μm/min at 435°C, faster by 0.27μm/min than mesas with PR at the same temperature. For both mesa structures, approximately parabolic behaviour is found for higher temperatures, but there is a different manner between the two geometry mesas for the initial growth. We explain this in Section 3.3.

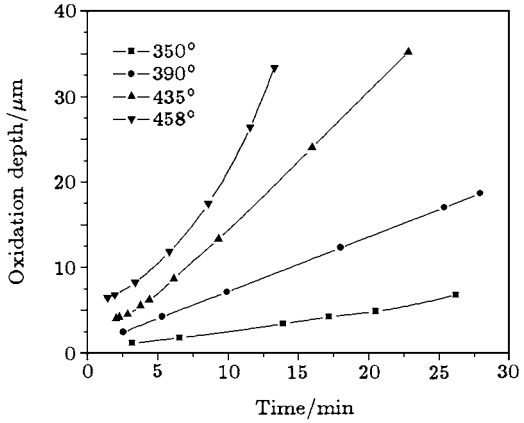

Fig.3. Measured selective oxidation depth versus time for mesas with RT at temperatures ranging from 350 to 458°C.

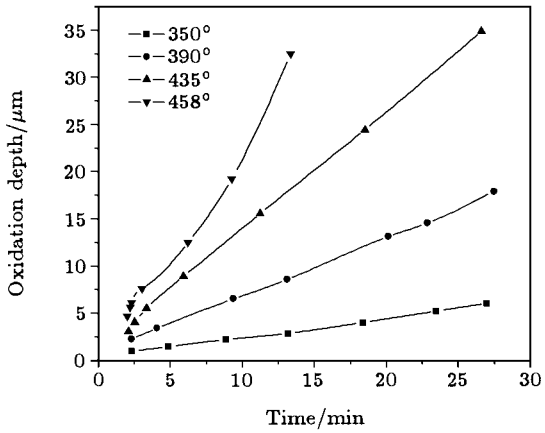

Fig.4. Measured selective oxidation depth versus time for mesas with PR at temperatures ranging from 350 to 458°C.

The selective oxidation is known to be very sensitive to temperature.[9,11] According to Fig.5, the selective oxidation rate increases with rising process temperature. Between 350°C and 435°C, the oxidation rate increases by a factor of 10. Therefore, higher temperatures result in a substantial reduction of the oxidation time which is necessary to produce a required oxide aperture.

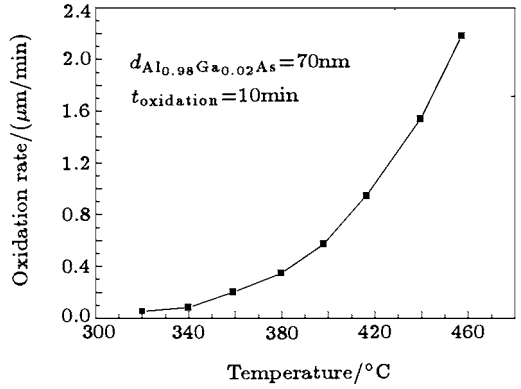

Fig.5. Plot of oxidation rate versus temperature for mesas with PR.

3.2. Dependence on N_2 carrier gas flow

Figure 6 shows the relationship between the carrier gas flow rate and the oxidation rate for 440°C. The water temperature was maintained at 92°C. The oxidation rate increases rapidly with increasing carrier gas flow rate in the small flow region. It then tends to become constant, independent of the carrier gas flow rate. The critical point is 1.27L/min. This means that in order to obtain an oxidation rate independent of the carrier gas flow rate, the carrier gas flow rate should be higher than 1.27L/min for 440°C. The critical gas flow rate increases for higher process temperature.

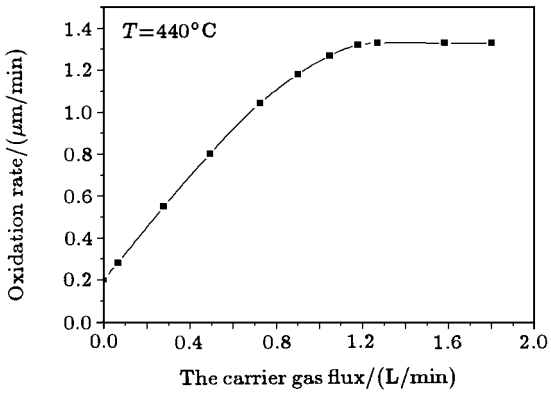

Fig.6. Plot of oxidation rate versus the carrier gas (N_2) flux for mesas with PR.

3.3. Dependence on geometry of the mesa structure

As shown in Fig.3 and Fig.4, at lower temperatures selective oxidation of $Al_{0.98}Ga_{0.02}As$ follows a linear growth law for the two mesa structures, and at higher temperatures approximately increasing parabolic growth is found. In both circles and squares, the surface area of the oxidation front decreases as the oxidation proceeds, and this geometric effect causes an increase in the oxidation rate.[12] However, at relatively low temperatures the thermal movement of ions and molecules (O_2^-,O_2,H_2O) is too slow to enable enough diffusion through the oxide. So geometry of the mesa structures has slight effect on oxidation rate. Conversely, there is an adequate supply of the reactant at the oxidation front at higher temperatures in spite of the increasing oxide length. Thus, we can see that geometry of mesa has a significant effect on the time dependence of the oxidation process at higher temperatures. For the mesa with RT, oxidation rate rises with increasing curvature of the oxidation front at higher temperatures. We would like to point out

that a similar effect is both expected and observed for the mesa with PR, another VCSEL configuration we employed, in spite of the different time dependence of the oxidation. In fact, from our experiment (shown in Fig.3 and Fig.4), the initial oxide growth of mesas with PR proceeds in a much different manner from that of mesas with RT. The observed difference between them can be explained theoretically as follows.

We take the oxidation time to be the sum of the time required for reactant atoms to diffuse into the oxide-semiconductor interface and the time required for the atoms to react at that interface:

$$t_{\text{oxidation}} = t_{\text{diffusion}}(D, x_0) + t_{\text{reaction}}(K, x_0). \quad (1)$$

Where K is the parameter relevant to the reaction rate, given by Eq.(3), D is the diffusion constant for oxygen in the oxide film. The oxidation time can also be expressed as[12]

$$t = \frac{x_0}{K} + \frac{x_0^2}{k_D}, \quad (2)$$

$$K = R/\rho\sigma, \quad (3)$$

$$k_D = 4D[\text{Erf}^{-1}(0.5)]^2. \quad (4)$$

where x_0 is the length of oxide formed, R is the reaction rate (in units of atoms per unit time), ρ is the concentration of oxidant molecules in the oxide, and σ is the outside surface area of oxidation front of the mesa. For lower temperatures k_D is very small and the second term on the right-hand side of Eq.(2)is very large, so K has no obvious effect on the total time t. Conversely, k_D is larger for higher temperatures and the first term in Eq.(2) contributes to the total time t obviously, i.e. the effect of K on the total time t cannot be ignored. For a steady-state process, we assume that R and ρ are constant at higher temperatures: i.e., independent on the distance from the interface with the ambient. In the case of mesas with RT ((a) of Fig.1), σ, the surface area of oxidation front, decreases as the oxidation proceeds. According to Eqs.(2) and (3), the oxidation rate increases as the oxidation front closes to the centre of the mesa. In the case of mesas with PR ((b) of Fig.1), the oxidation toward the centre of the mesa starts from multiple separated holes. Thus σ increases for the initial oxidation until multiple separated oxidation fronts get touched and decreases as the oxidation proceeds, leading to the curve of oxidation rate going down for the first minutes and then going up for the rest of the time. Therefore, we can see the geometry of mesa structures distinctly influence the oxide growth rate at higher temperatures.

4. Conclusion

We present results of our studies of lateral oxidation of $Al_{0.98}Ga_{0.02}As$ layers in VCSEL structures. The oxidation follows an approximately linear behaviour for lower temperatures (below 435°C) and increasing parabolic behaviour for higher temperatures. The selective oxidation rate increases with rising process temperature. Between 350°C and 435°C, the oxidation rate increases by a factor of 10. From the different manner between the two geometry mesas(RT and PR) for the initial growth, we demonstrate that the geometry of mesa structures distinctly influences the oxide growth rate at higher temperatures.

References

[1] Pan Z, Wu R H and Wang Q M 1995 *Acta Phys. Sin.* **4** 810 (in Chinese)

[2] Choquette K D, Geib K M and Ashby C I H 1997 *IEEE J. Select. Topics Quantum Electron* **3** 916

[3] MacDougal M H, Dapkus P D and Pudikov V 1995 *IEEE Photon. Technol. Lett.* **7** 229

[4] Li H Q, Zhang J, Cui D F, Xu Z Y, Ning Y Q, Yan C L, Qin L, Liu Y, Wang L J and Cao J L 2004 *Acta Phys. Sin.* **53** 2986 (in Chinese)

[5] Lear K L, Choquette K D, Schneider R P, Kilcoyne S P and Geib K M 1995 *Electron Lett.* **31** 208

[6] Yue A W, Zhang W, Zhan D P, Wang R F, Shen K and Shi J 2003 *Chin. J. Semicond.* **24** 693

[7] Osinski M, Svimonishvili T, Smolyakov G A , Smagley V A, kowiak P M and Nakwaski W 2001 *IEEE Photon. Technol. Lett.* **13** 687

[8] Choquette K D, Lear K L, Schneider R P, Geib K M, Figiel J J and Hull R 1995 *IEEE Photon. Technol. Lett.* **7** 1237

[9] Ochiai M, Giudice G E, Temkin H, Scott J W and Cockerill T M 1996 *Appl. Phys. Lett.* **68** 1898

[10] Hao Y Q, Zhong J C, Xie H R, Jiang X G, Zhao Y J and Wang L J 2005 *Chin. J. Semicond.* **26** 2290

[11] Zhang Y, Pan Z, Du Y, Huang Y J and Wu R H 1999 *Chin. J. Semicond.* **20** 260

[12] Alonzo A C, Ceng X C and McGill T C 1998 *J. Appl. Phys.* **84** 6901